Thermal expansion, compressibility and volumetric changes of quartz obtained by single crystal dilatometry to 700 °C and 3.5 kilobar (0.35 GPa)

Autor(en): **Raz, Urs / Girsperger, Sven / Thompson, Alan Bruce**

Objekttyp: **Article**

Zeitschrift: **Schweizerische mineralogische und petrographische Mitteilungen = Bulletin suisse de minéralogie et pétrographie**

Band (Jahr): **82 (2002)**

Heft 3

PDF erstellt am: **26.04.2024**

Persistenter Link: https://doi.org/10.5169/seals-62381

SCHWEIZ. MINERAL. PETROGR. MITT. 82, 561–574, 2002

Thermal expansion, compressibility and volumetric changes of quartz obtained by single crystal dilatometry to 700 °C and 3.5 kilobar (0.35 GPa)

by *Urs Raz*[1,2], *Sven Girsperger*[1] and *Alan Bruce Thompson*[1]

Abstract

A dilatometer has been developed to measure volumetric changes of oriented single crystals simultaneously as a function of pressure and temperature to 0.6 GPa and 900 °C. Argon gas is used as the pressure medium inside an externally heated hydrothermal cold-seal rod-bomb. The present apparatus has been used to measure thermal expansion of quartz in the two principal crystallographic directions as a function of pressure to 0.35 GPa, 700 °C. Thermal expansion for directions parallel to a(x) and c(z) increases with increasing temperature, and increases very sharply close to the low-high-quartz transition. High-quartz shows negative thermal expansion. The linear compressibility of low-quartz is greater in the direction parallel to c(z) than it is parallel to a(x), at least to 0.35 GPa. The measured data have been fitted to an Equation Of State (EOS) and can be used to determine the volume and directional length changes of single crystals of quartz in piezothermometric devices, in other industrial applications, as well as in measurement sensors in natural volcanic and hydrothermal systems.

Keywords: quartz, thermal expansion, compressibility, dilatometer, equation of state.

1. Introduction

For the calculation of phase equilibria involving extrapolation over large ranges in pressure and temperature relevant to conditions inside the Earth and other planets, thermodynamic data need to be measured as accurately as possible. Unfortunately their measurement is a tedious and technically demanding task especially at elevated pressures and temperatures. Consequently the data bases for thermal properties of minerals (heat of formation, specific heat, latent heat), as well as thermoelastic properties (density, reactive volume), have grown quite slowly.

In recent years micro-scale specimens in diamond anvils and solid media cells mounted in synchrotron beams for x-ray diffraction work, have been used to determine crystal structures and sometimes volumetric properties of minerals at elevated temperatures and pressure. While techniques for crystal structure determinations have certainly improved in recent years (see D'AMOUR et al., 1979; LEVIEN et al., 1980; GLINNEMAN et al., 1992; ANGEL et al., 1997; OGATA et al., 1987), pressure and temperature control in such devices is not very precise (see MILETICH, 2000). Furthermore in such microscopic devices, directional thermal expansion and compression data must be obtained from unit cell measurements and only small scale samples (<10 μm) can be used. Measurement techniques on meso-scale samples (mm to cm) have advanced very little since the pioneering work of P.W. BRIDGMAN (1948 a and b, 1949). Our study presents a new dilatometer for direct measurement of length change of single crystals at elevated pressure and temperature, with corresponding data for meso-scale crystals of quartz.

While our method imposes limitations in terms of specimen type (need for large and disorder-free single crystals) and P-T-range (correspondingly spacious experimental chamber required), our type of experiment may be run with straightfor-

[1] Department of Earth Sciences, ETH-Zentrum, CH-8092 Zürich, Switzerland. <sven.girsperger@erdw.ethz.ch> <alan.thompson@erdw.ethz.ch>
[2] Solexperts AG, Schulstrasse 5, CH-8603 Schwerzenbach, Switzerland. <urus@bluewin.ch>

ward basic hydrothermal pressure-temperature equipment (cold seal rod-bomb). In addition, it provides superior accuracy and resolution for volumetric measurements, because it permits direct determination of directional length change (α - directional expansion, β - directional compressibility) as a function of simultaneous changes in pressure and temperature on crystals of industrial size.

2. Previous volumetric data for quartz as functions of pressure and temperature

The structure of low-quartz can be viewed as a distortion of that of high-quartz (HEANEY et al., 1994, p. 6). The low-quartz structure (with a space group of $P3_121$ for left-handed and $P3_221$ for right-handed twins) consists of two sets of chains of SiO_4 tetrahedra forming spirals parallel to the c-axis (HEANEY et al., 1994, p. 9; HEMLEY et al., 1994, p. 43).

A recent comparison of the P–V equations of state for various silica polymorphs at room temperature (near 300 K, see HEMLEY et al., 1994, p. 49, Fig. 4) summarises for low-quartz the measured continuous decrease in molar volume with increasing pressure[1].

The thermal expansion (α) for most silica polymorphs has only been measured at ambient pressure (1 bar).

Three simultaneous mechanisms permit the quartz structure to decrease in volume with increasing pressure, (1) distortion of tetrahedra in response to changes in bond angle, (2) decrease in bond length, but mainly (3) rotation of linked tetrahedra (JORGENSEN, 1978). Changes in the Si–O–Si angle and the tetrahedral tilt angle control the thermal expansion, whereas smaller changes in the Si–O–Si angle and the tetrahedral distortion control isothermal compression (D'AMOUR et al., 1979; LEVIEN et al., 1980).

2.1. VOLUMETRIC DATA MEASURED IN SITU AT P AND T

Traditionally, hydrothermal experimentation techniques rely on quenching before samples can be examined. In quenching methods, starting materials (solids and liquids) are hermetically enclosed in a chemically inert container and taken to pressure P and temperature T. The selected P-T-conditions are maintained for a duration deemed long enough for the expected reaction to fully take place, typically hours to months. Subsequently, the sample is returned to ambient conditions as rapidly as possible in order to 'freeze' the phases that were stable at P and T, thus allowing the experimenter to remove and examine the products of the reaction. Obviously this procedure is unsuitable for the measurement of ther-

[1] Because the symbol α is often used to denote the thermal expansion coefficient, as well as the low temperature form of quartz (α-quartz) we generally refer to this form as *low-quartz* here.

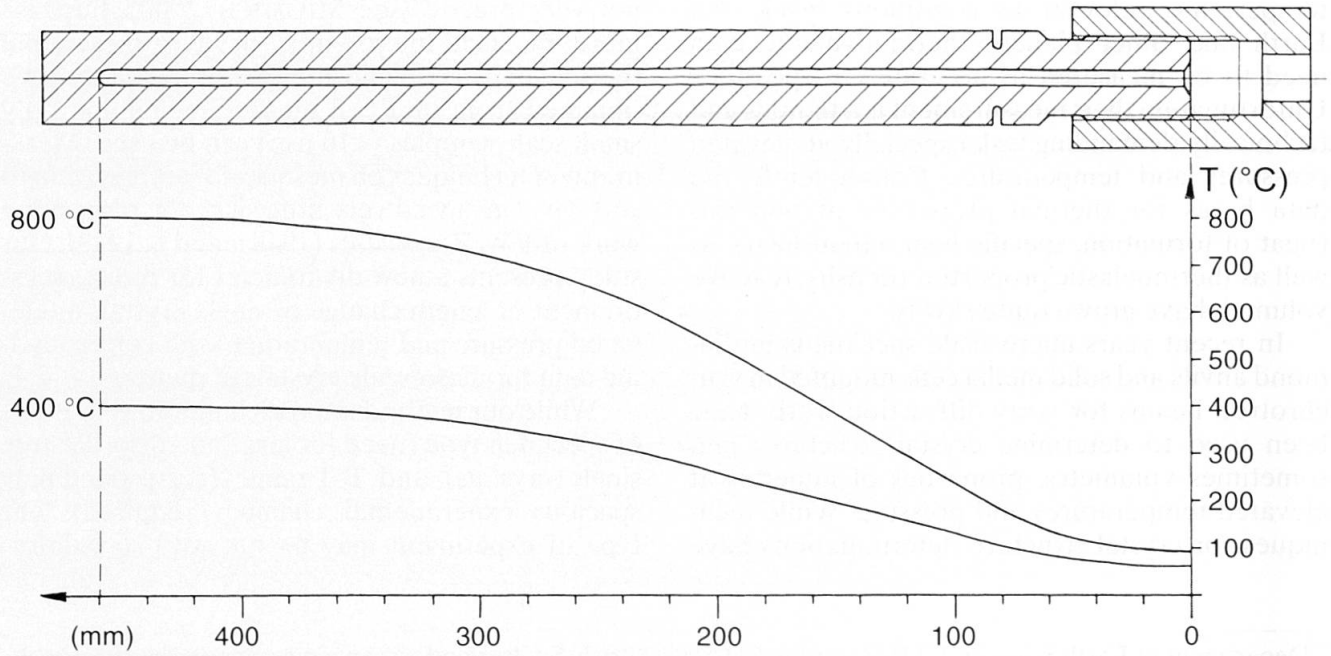

Fig. 1 Axial temperature gradient in pressure vessel at 400 and 800 °C at 1 bar. Samples are placed near the closed end of the bore hole where a thermal gradient of less than 1 °C over 20 mm is attained.

modynamic data at P and T. The properties in question are not quenchable and must be studied in situ at P and T. We therefore needed to develop procedures to perform relative and absolute metric measurements inside an experimental chamber at P and T.

Apparatus constraints, such as diminishing material strength at increasing temperatures, finite overall hardness and tensile strength, limit our type of measurement to a maximum of about 15 kbar (1.5 GPa) and 1000 °C in internally heated pressure vessels. Higher gas pressures are extremely difficult to seal routinely and gas is required as the pressurizing medium to ensure isostatic shear-free conditions. Externally heated vessels (cold seal rod-bombs), as used in this study, are limited to about 7 kbar and 900 °C. However, in the cold seal type apparatus the metal rapidly loses strength with rising temperature. It is thus unsuitable to follow normal geothermal gradients where temperature and pressure increase simultaneously (the tensile strength of alloys used for cold seal bombs drops off sharply at approx. 500 °C).

Our apparatus allows both pressure and temperature scans; i.e. compressibility with increasing temperature and thermal expansion with increasing pressure may be measured directly. In terms of pressure and temperature, the scan range and direction (up or down P and T) be may be chosen without restriction. This feature proved to be extremely helpful for the volumetric and kinetic study of phase transitions (experiments of this type will be discussed in another paper).

In comparison, micro volume diamond anvil cells do offer a vast pressure range up to 300 GPa, but usually at room temperature. Thus such experimentation still lacks a reliable and accurate pressure scale covering this P-T range, especially when the diamond cells are laser-heated to attain elevated temperatures. Data obtained by anvil cells still need to be considered to have limited metric accuracy and resolution, especially when extended to higher temperatures either by internal or external heating.

3. Design of apparatus and control of temperature and pressure

A conventional cold seal type externally heated pressure vessel has been modified for this study. In order to achieve a reasonably large isothermal zone, the bomb design was changed from the routinely used length of 250 mm to 500 mm. This, together with appropriately distributed electric heating power of the furnace resulted in an axial thermal gradient of less than 1 °C over 20 mm at the stationary hot spot for all temperatures up to 900 °C (Fig. 1).

The thermal gradient was established in a special cold seal type externally heated pressure vessel containing six equally spaced thermocouples at pressures up to 6 kbar. It turned out to be independent of pressure down to ambient conditions. It was found however, that the location of the smallest thermal gradient shifted with changing heating and cooling rate. Therefore, the location of the bombs within the furnace had to be shifted according to the actual rate of temperature change chosen for a given experiment. The radial temperature gradient is assumed to be negligible. The pressurizing medium was Argon gas of 99.999% purity (technical term: Argon 5.0).

Argon gas from commercial bottles at a maximum pressure of 200 bar was pressurized in two steps up to a maximum of 6.5 kbar. A commercial air driven two-stage membrane pump was used up to 3.0 kbar, whereas higher pressures were attained with a 1:10 intensifier driven by a small piston water pump on the low pressure side. For safety, and economic reasons, the dead volume (= pressurized gas volume) of the entire system was kept as small as practical by using either 1/16" capillary tubing (ID = 0.1 mm) or 1/8" tubing (ID = 0.5 mm). The typical dead volume in a bomb set up for experimentation was 1.5 to 2 cm^3.

Pressures were routinely measured with strain-gauge type and piezo-electric transducers having a resolution of 200 mbar and 20 mbar at 7 kbar at full scale, respectively. This is to say that, at 200 or 20 mbar, the signal started to disappear in amplifier electronic noise. These pressure readings were compared to Bourdon type gauges (manufactured by Heise) with a resolution of 5 bar (= 1 division on the dial). Hysteresis of the beryllium alloy Bourdon tubes was remarkably low (5 to 10 bar maximum even after long duration, days to weeks, near full-scale excursions above 6 kbar). The gauges were calibrated against secondary standards (I-II phase transition of ammonium fluoride (KANEDA et al., 1971), low-high-quartz transition). A primary dead weight tester calibration was not available. Scale linearity between the calibration points is assumed. Pressures are considered accurate to +/–15 bar.

Temperatures were measured with type-K Inconel sheathed thermocouples inside the bomb by means of brazed pressure feed-throughs. Hot junctions were kept fully isolated from the ground to avoid inductive noise stemming mainly from the 50 Hz AC power line feeding the heating coils. A conventional water–ice bath in a Dewar flask served as the cold junction. Thermocouples were

calibrated against a type-S Pt-Rh laboratory standard which itself was verified at the Swiss Federal Institute of Standards in Bern. Comparison of the working type-K thermocouples with the standard type-S thermocouple was performed in a special calibration furnace under computer control. Temperatures are considered accurate to +/–2 °C, whereas temperature resolution is below 0.5 °C.

Furnace temperatures were kept to the set value by means of PID (Proportional Integral Differential) controllers driving two AC-line half-wave thyristors. This technique was preferred to phase-angle control in order to prevent injection of spurious noise into the AC line, which interferes unfavorably with the measuring computers. Set values were changed under computer control by adding a time dependent offset voltage to the

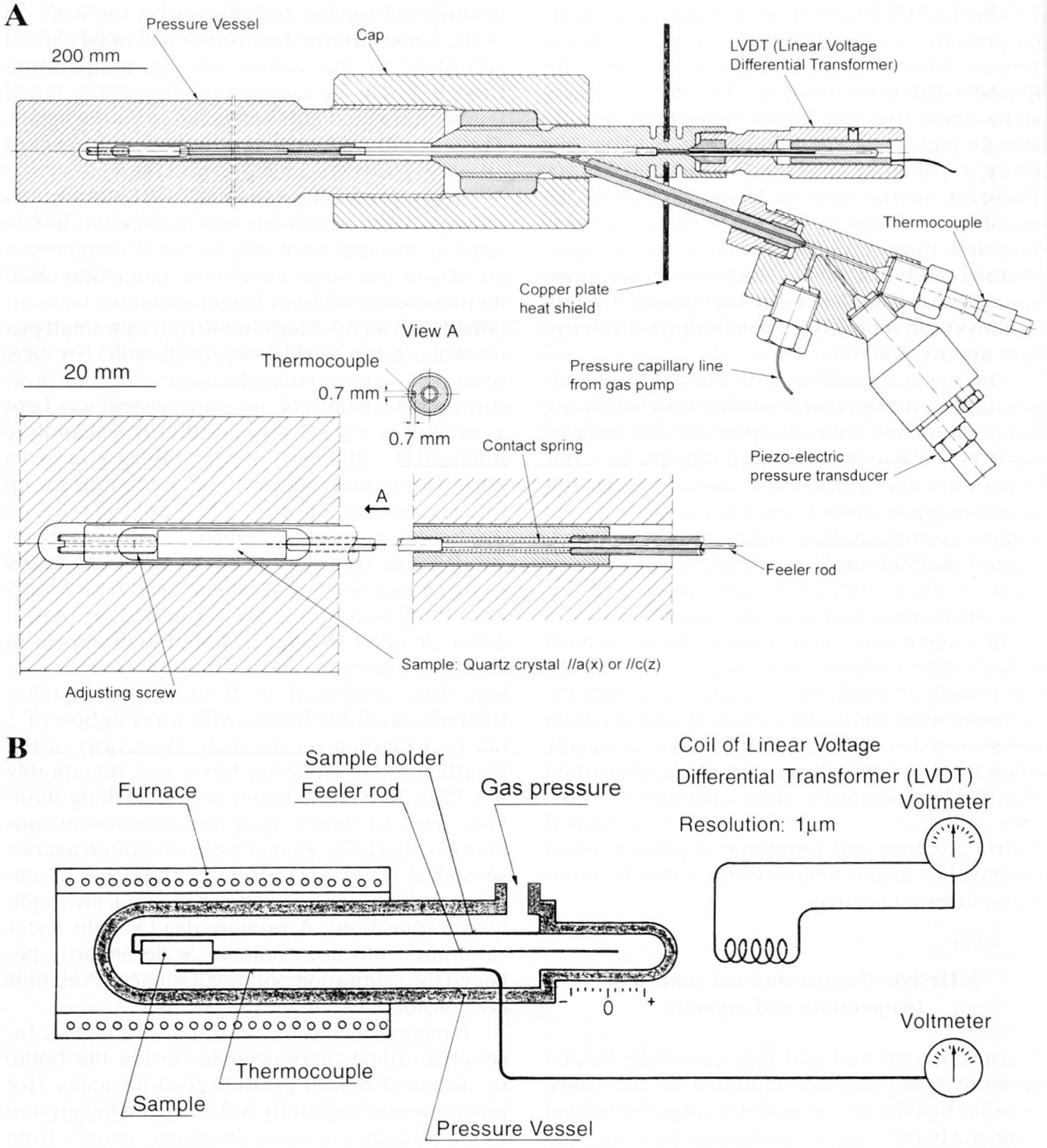

Fig. 2 (A) Engineering drawing of pressure vessel with dilatometer, LVDT, thermocouple and piezo-electric pressure transducer. (B) Schematic layout of dilatometer. Both feeder rod and sample holder are manufactured from the same batch of AIAI 316 stainless-steel in order to fully compensate relative thermo-elastic response.

controller's sensing thermocouple (also called generation of temperature "ramps").

Pressures were set by manually-operated shut-off valves. Thermally induced pressure changes followed the coefficient $(\delta p/\delta T)V$ for Argon (isochoric temperature induced pressure change). In a later addition to the apparatus, a computer controlled bleed valve allowed us to decrease pressure in steps of approx. 2 to 5 bar starting at 6.5 kbar.

The dilatometer option (Fig. 2) in the pressure vessels was made up in a conventional way by a

Table 3 The interpolated data set for the PVT properties of quartz single crystals, given as molar volume (in cm^3), as dV/V_0 in percent, (dl_x/dl_{0x}) and (dl_z/dl_{0z}) in percent; Pressures given in bars, temperatures in degrees Celsius.

Pressure (bar)	Temp. (°C)	(V(P,T) (cm^3)	dV/V_0 (%)	dlx/dlx0 (%)	dlz/dlz0 (%)
3000	25	22.5163	–0.7567	–0.2890	–0.1806
3000	100	22.5881	–0.4405	–0.1673	–0.1065
3000	200	22.6834	–0.0202	–0.0081	–0.0040
3000	300	22.7827	0.4174	0.1541	0.1086
3000	400	22.8985	0.9276	0.3478	0.2292
3000	500	23.0469	1.5818	0.5929	0.3879
3000	520	23.0798	1.7268	0.6487	0.4197
3000	540	23.1202	1.9049	0.7210	0.4512
3000	560	23.1622	2.0899	0.7933	0.4892
3000	580	23.2007	2.2598	0.8640	0.5154
3000	600	23.2479	2.4679	0.9393	0.5697
3000	610	23.2775	2.5984	0.9887	0.5993
3000	620	23.3092	2.738	1.0424	0.6291
3000	630	23.3481	2.9093	1.1105	0.6612
3000	640	23.3930	3.1073	1.1911	0.6943
3000	650	23.4511	3.3632	1.3000	0.7273
2600	25	22.5407	–0.6494	–0.2466	–0.1576
2600	100	22.6115	–0.3370	–0.1270	–0.0834
2600	200	22.7077	0.0869	0.0333	0.0203
2600	300	22.8087	0.5320	0.1986	0.1339
2600	400	22.9258	1.0481	0.3942	0.2561
2600	500	23.0780	1.7189	0.6466	0.4161
2600	520	23.1117	1.8677	0.7042	0.4480
2600	540	23.1540	2.0538	0.7787	0.4828
2600	560	23.1973	2.2449	0.8533	0.5221
2600	580	23.2371	2.4203	0.9269	0.5477
2600	600	23.2909	2.6573	1.0135	0.6076
2600	610	23.3230	2.7987	1.0667	0.6402
2600	620	23.3594	2.9594	1.1291	0.6732
2600	630	23.4043	3.1572	1.2096	0.7062
2600	640	23.4663	3.4307	1.3271	0.7391
2600	650	23.6089	4.0590	1.5987	0.8099
2400	25	22.5513	–0.6023	–0.2283	–0.1469
2400	100	22.6230	–0.2864	–0.1072	–0.0723
2400	200	22.7199	0.1407	0.0341	0.0324
2400	300	22.8209	0.5857	0.2190	0.1466
2400	400	22.9397	1.1095	0.4185	0.2683
2400	500	23.0937	1.7884	0.6731	0.4318
2400	520	23.1284	1.9410	0.7321	0.4646
2400	540	23.1711	2.1292	0.8080	0.4986
2400	560	23.2152	2.3236	0.8840	0.5382
2400	580	23.2572	2.5088	0.9614	0.5658
2400	600	23.3136	2.7575	1.0522	0.6287
2400	610	23.3476	2.9073	1.1084	0.6634
2400	620	23.3874	3.0826	1.1768	0.6986
2400	630	23.4397	3.3132	1.2722	0.7338
2400	640	23.6333	4.1667	1.6118	0.8882
2400	650	23.6335	4.1676	1.6100	0.8927

All Tables including Table 1 and 2 are available in electronic form from our website: http://e-collection.ethbib.ethz.ch/show?type=bericht&nr=184

Table 3 (continued)

Pressure (bar)	Temp. (°C)	(V(P,T) (cm^3)	dV/V_0 (%)	dlx/dlx0 (%)	dlz/dlz0 (%)
2200	25	22.5631	–0.5506	–0.2087	–0.1342
2200	100	22.6348	–0.2344	–0.0874	–0.0598
2200	200	22.7325	0.1963	0.0756	0.0450
2200	300	22.8354	0.6497	0.2445	0.1593
2200	400	22.9535	1.1700	0.4419	0.2818
2200	500	23.1087	1.8541	0.6979	0.4472
2200	520	23.1439	2.0092	0.7577	0.4808
2200	540	23.1882	2.2047	0.8366	0.5158
2200	560	23.2339	2.4062	0.9155	0.5566
2200	580	23.2776	2.5988	0.9962	0.5848
2200	600	23.3378	2.8642	1.0939	0.6501
2200	610	23.3745	3.0260	1.1546	0.6875
2200	620	23.4184	3.2192	1.2302	0.7257
2200	630	23.4823	3.5011	1.3491	0.7639
2200	640	23.6430	4.2095	1.6261	0.9013
2200	650	23.6436	4.2121	1.6255	0.9050
2000	25	22.5743	–0.5010	–0.1900	–0.1218
2000	100	22.6464	–0.1833	–0.0683	–0.0468
2000	200	22.7434	0.2530	0.0971	0.0586
2000	300	22.8475	0.7030	0.2636	0.1742
2000	400	22.9669	1.2293	0.4628	0.2988
2000	500	23.1250	1.9259	0.7253	0.4633
2000	520	23.1608	2.0840	0.7863	0.4973
2000	540	23.2061	2.2838	0.8672	0.5326
2000	560	23.2530	2.4904	0.9480	0.5745
2000	580	23.2989	2.6925	1.0326	0.6041
2000	600	23.3626	2.9734	1.1360	0.6731
2000	610	23.4028	3.1505	1.2023	0.7142
2000	620	23.4548	3.3798	1.2934	0.7566
2000	630	23.6410	4.2006	1.6177	0.9094
2000	640	23.6494	4.2375	1.6341	0.9125
2000	650	23.6528	4.2523	1.6398	0.9155
1800	25	22.5860	–0.4495	–0.1709	–0.1084
1800	100	22.6575	–0.1346	–0.0502	–0.0343
1800	200	22.7566	0.3024	0.1149	0.0723
1800	300	22.8616	0.7650	0.2874	0.1883
1800	400	22.9826	1.2985	0.4883	0.3164
1800	500	23.1411	1.9972	0.7523	0.4797
1800	520	23.1781	2.1601	0.8151	0.5148
1800	540	23.2247	2.3654	0.8984	0.5506
1800	560	23.2730	2.5785	0.9816	0.5939
1800	580	23.3207	2.7889	1.0699	0.6242
1800	600	23.3886	3.0880	1.1805	0.6965
1800	610	23.4318	3.2784	1.2550	0.7341
1800	620	23.4755	3.4710	1.3304	0.7718
1800	630	23.6193	4.1048	1.6014	0.8490
1800	640	23.6531	4.2537	1.6463	0.9040
1800	650	23.6601	4.2847	1.6501	0.9265

sample holder and a spring loaded feeler-rod, both manufactured from the same material (AISI 316 stainless-steel) in order to cancel out their relative thermo-elastic response.

4. Measurement procedures

Movement of the feeler rod was sensed electromagnetically through the walls of a piece of pressure tubing located inside the coil of a conventional LVDT (Linear Voltage Differential Transformer). Stainless steel tubing of AISI 304 or 316 grades turned out to dampen the LVTD signal the least. With this arrangement, resolution was below 1 μm and limited only by electronic amplifier noise. The LVDT's amplified signal was calibrated with a micrometer allowing readings down to 1μm. This technique of taking metric length measurements inside a pressurized container without the

Table 3 (continued)

Pressure (bar)	Temp. (°C)	(V(P,T) (cm^3)	dV/V_0 (%)	dlx/dlx0 (%)	dlz/dlz0 (%)
1600	25	22.5978	–0.3976	–0.1512	–0.0957
1600	100	22.6697	–0.0806	–0.0298	–0.0210
1600	200	22.7689	0.3566	0.1350	0.0862
1600	300	22.8745	0.8219	0.3086	0.2025
1600	400	22.9961	1.3579	0.5102	0.3315
1600	500	23.1579	2.0710	0.7805	0.4961
1600	520	23.1957	2.2376	0.8447	0.5320
1600	540	23.2434	2.4482	0.9299	0.5691
1600	560	23.2928	2.6656	1.0150	0.6128
1600	580	23.3436	2.8896	1.1085	0.6439
1600	600	23.4182	3.2187	1.2316	0.7224
1600	610	23.4665	3.4315	1.3159	0.7622
1600	620	23.6538	4.2567	1.6365	0.9263
1600	630	23.6611	4.2889	1.6504	0.9299
1600	640	23.6660	4.3107	1.6592	0.9335
1600	650	23.6679	4.3192	1.6618	0.9366
1400	25	22.6088	–0.349	–0.1335	–0.0824
1400	100	22.6811	–0.0304	–0.0114	–0.0076
1400	200	22.7815	0.4119	0.1560	0.0994
1400	300	22.8872	0.8779	0.3295	0.2164
1400	400	23.0103	1.4208	0.5336	0.3470
1400	500	23.1735	2.1401	0.8065	0.5123
1400	520	23.2121	2.3099	0.8716	0.5495
1400	540	23.2614	2.5273	0.9603	0.5862
1400	560	23.3129	2.7544	1.0489	0.6323
1400	580	23.3671	2.9934	1.1486	0.6676
1400	600	23.4488	3.3533	1.2834	0.7506
1400	610	23.4960	3.5615	1.3637	0.7937
1400	620	23.6514	4.2462	1.6240	0.9410
1400	630	23.6700	4.3281	1.6631	0.9426
1400	640	23.6740	4.3459	1.6710	0.9442
1400	650	23.6748	4.3495	1.6715	0.9466
1200	25	22.6210	–0.2951	–0.1128	–0.0698
1200	100	22.6936	0.0246	0.0093	0.0060
1200	200	22.7937	0.4660	0.1755	0.1143
1200	300	22.9003	0.9358	0.3511	0.2308
1200	400	23.0248	1.4847	0.5575	0.3625
1200	500	23.1914	2.2188	0.8365	0.5299
1200	520	23.2311	2.3936	0.9038	0.5675
1200	540	23.2818	2.6172	0.9953	0.6046
1200	560	23.3350	2.8515	1.0868	0.6519
1200	580	23.3932	3.1082	1.1932	0.6910
1200	600	23.4854	3.5148	1.3462	0.7831
1200	610	23.6692	4.3247	1.6569	0.9517
1200	620	23.6748	4.3496	1.6685	0.9527
1200	630	23.6780	4.3635	1.6748	0.9536
1200	640	23.6822	4.3822	1.6835	0.9545
1200	650	23.6830	4.3856	1.6840	0.9567

Table 3 (continued)

Pressure (bar)	Temp. (°C)	(V(P,T) (cm^3)	dV/V_0 (%)	dlx/dlx0 (%)	dlz/dlz0 (%)
1000	25	22.6339	–0.2383	–0.0913	–0.0559
1000	100	22.7057	0.0779	0.0291	0.0197
1000	200	22.8059	0.5195	0.1953	0.1280
1000	300	22.9135	0.9940	0.3726	0.2456
1000	400	23.0397	1.5501	0.5821	0.3781
1000	500	23.2087	2.2950	0.8659	0.5462
1000	520	23.2491	2.4733	0.9347	0.5842
1000	540	23.3024	2.7078	1.0302	0.6239
1000	560	23.3579	2.9528	1.1257	0.6735
1000	580	23.4211	3.2314	1.2416	0.7149
1000	600	23.5306	3.7140	1.4241	0.8219
1000	610	23.6526	4.2517	1.6553	0.8842
1000	620	23.6800	4.3723	1.6826	0.9466
1000	630	23.6862	4.3998	1.6872	0.9641
1000	640	23.6896	4.4145	1.6939	0.9650
1000	650	23.6901	4.4169	1.6941	0.9670
800	25	22.6453	–0.1884	–0.0725	–0.0433
800	100	22.7177	0.131	0.0495	0.0319
800	200	22.8187	0.5761	0.2162	0.1426
800	300	22.9267	1.0519	0.3942	0.2599
800	400	23.0548	1.6166	0.6067	0.3947
800	500	23.2261	2.3716	0.8953	0.5629
800	520	23.2671	2.5527	0.9651	0.6015
800	540	23.3231	2.7992	1.0654	0.6433
800	560	23.3814	3.0562	1.1657	0.6949
800	580	23.4519	3.3671	1.2944	0.7422
800	600	23.6815	4.379	1.6848	0.9488
800	610	23.6858	4.3978	1.6885	0.9596
800	620	23.6919	4.4248	1.6962	0.9704
800	630	23.6935	4.4317	1.6979	0.9737
800	640	23.6961	4.4432	1.7032	0.9743
800	650	23.6980	4.4518	1.7063	0.9765
600	25	22.6576	–0.1338	–0.0518	–0.0303
600	100	22.7303	0.1865	0.0705	0.0454
600	200	22.8312	0.6311	0.2371	0.1556
600	300	22.9408	1.1144	0.4180	0.2744
600	400	23.0700	1.6838	0.6322	0.4102
600	500	23.2444	2.4525	0.9263	0.5805
600	520	23.2870	2.6403	0.9987	0.6205
600	540	23.3458	2.8994	1.1042	0.6641
600	560	23.4071	3.1696	1.2098	0.7179
600	580	23.4681	3.4385	1.3153	0.7702
600	600	23.6864	4.4006	1.6880	0.9633
600	610	23.6955	4.4406	1.7031	0.9720
600	620	23.6998	4.4595	1.7080	0.9806
600	630	23.7025	4.4714	1.7123	0.9835
600	640	23.7038	4.4770	1.7146	0.9844
600	650	23.7051	4.4829	1.716	0.9873

need for electrical or mechanical feed-throughs turned out to be a key factor for the overall success of this study.

Control of the experiments (temperature ramps and cycles, stepwise pressure bleed off) and all data acquisition was accomplished with DEC PDP-11 computers running the RT-11 operating system (Foreground-Background monitor). Voltages from thermocouples, LVDT amplifiers and pressure transducers were scanned with a low thermal-offset reed-relay scanner (HP 3495A) and routed to a digital voltmeter (HP 3456A). For instrument control, the HP-IB / IEEE-488 bus was used. Bias voltages driving temperature ramps were generated by a programmable digital to analog power supply (HP 59501A) and suitably arranged voltage-dividing resistors.

Table 3 (continued)

Pressure (bar)	Temp. (°C)	(V(P,T) (cm^3)	dV/V_0 (%)	dlx/dlx0 (%)	dlz/dlz0 (%)
400	25	22.6686	–0.0855	–0.0336	–0.0183
400	100	22.7421	0.2383	0.0899	0.0583
400	200	22.8445	0.6896	0.2589	0.1703
400	300	22.9542	1.1732	0.4397	0.2893
400	400	23.0857	1.7529	0.6581	0.4267
400	500	23.2635	2.3367	0.9581	0.5998
400	520	23.3072	2.7291	1.0323	0.6405
400	540	23.3698	3.0050	1.1449	0.6863
400	560	23.4353	3.2939	1.2575	0.7442
400	580	23.5015	3.5857	1.3701	0.8045
400	600	23.7036	4.4764	1.7180	0.9770
400	610	23.7054	4.4841	1.7178	0.9849
400	620	23.7089	4.4996	1.7214	0.9927
400	630	23.7110	4.5089	1.7245	0.9955
400	640	23.7123	4.5146	1.7268	0.9965
400	650	23.7133	4.5192	1.7277	0.9991
200	25	22.6803	–0.0338	–0.0145	–0.0048
200	100	22.7546	0.2934	0.1107	0.0717
200	200	22.8589	0.7531	0.2830	0.1852
200	300	22.9706	1.2455	0.4670	0.3064
200	400	23.1040	1.8336	0.6888	0.4451
200	500	23.2846	2.6298	0.9932	0.6211
200	520	23.3300	2.8298	1.0706	0.6629
200	540	23.3977	3.1279	1.1927	0.7112
200	560	23.4684	3.4398	1.3148	0.7725
200	580	23.6743	4.3472	1.7209	0.8464
200	600	23.7121	4.5138	1.7348	0.9798
200	610	23.7163	4.5323	1.7345	0.9983
200	620	23.7192	4.5451	1.7374	1.0049
200	630	23.7210	4.5531	1.7401	1.0073
200	640	23.7221	4.5580	1.7420	1.0082
200	650	23.7229	4.5614	1.7422	1.0111
1	25	22.6929	0.0215	0.0074	0.0067
1	100	22.7671	0.3488	0.1316	0.0852
1	200	22.8710	0.8065	0.3025	0.1994
1	300	22.9836	1.3028	0.4887	0.3199
1	400	23.1212	1.9094	0.7173	0.4630
1	500	23.3067	2.7270	1.0311	0.6409
1	520	23.3537	2.9340	1.1114	0.6836
1	540	23.4272	3.2581	1.2448	0.7346
1	560	23.5043	3.5981	1.3781	0.8007
1	580	23.7134	4.5197	1.7418	0.9716
1	600	23.7266	4.5779	1.7540	1.0036
1	610	23.7286	4.5867	1.7543	1.0115
1	620	23.7312	4.5981	1.1569	1.0174
1	630	23.7322	4.6024	1.7575	1.0203
1	640	23.7339	4.6101	1.7604	1.0220
1	650	23.7355	4.6168	1.7623	1.0247

5. Results of PVT measurements

Three samples of quartz were used for the investigation of its volumetric properties and the low/high transition at pressures up to 3.5 kbar:

(1) clear, colorless vein quartz (used for the development of the method)
(2) synthetic quartz cut parallel to the c(z)-axis
(3) smoky vein quartz cut parallel to the a(x)-axis

The samples were cut into cylindrical pieces of about 25 mm length and 5 mm OD, resulting in an overall weight of 1.5–2 g. A 0.8 mm hole was drilled half way along the cylinder axis to accommodate a 0.5 mm OD sheathed thermocouple. In accordance with earlier studies, the phase boundary between low and high-quartz proved to follow a straight line up to 3.5 kbar (Figs. 3, 4, 5 and Tables 1, 2, 3).

Our linear isothermal compressibility parallel a(x) and parallel c(z) deviates from those measured by BRIDGMAN (1948), see Fig. 3. Initially this difference was attributed to argon gas that had diffused into the crystal. To further investigate this effect we ran the same experiments with helium and nitrogen as the pressure medium. These runs yielded essentially the same differences and thereby practically ruled out the diffusion hypothesis. In order to suppress gas diffusion into the crystal lattice, future experiments could be carried out with gold plated/encapsulated samples because in another set of experiments gold turned out to be impermeable to argon and helium at these high pressures and temperatures.

6. Equations of State and fitting of PVT data

The α-quartz structure (with a space group of $P3_121$) consists of two sets of chains of SiO_4 tetrahedra forming spirals parallel to the c(z)-axis (HEMLEY et al., 1994, p. 43). The deformation of these tetrahedral chains is reflected by the dilatometric measurements. The linear thermal expansion and compressibility of quartz parallel to the crystallographic a(x)- and c(z)-axis were measured in the range up to 3.5 kbar and to 640 °C.

Thermal expansion agrees well with the data of SKINNER (1966), JAY (1933) and MAYER (1960) in showing also negative thermal expansion for high-quartz. Compressibility measurements at room temperature are consistent with the results of BRIDGMAN (1948 a and b; 1949) but show increased compressibility parallel to c(z) above about 2 kbar and for parallel to a(x) above about 3 kbar. Relative changes in length as a function of pressure and temperature are shown in Fig. 4. These data (see link to website in Table 3) were used to calculate an interpolated set of volumetric properties (Table 3) for a given P and T.

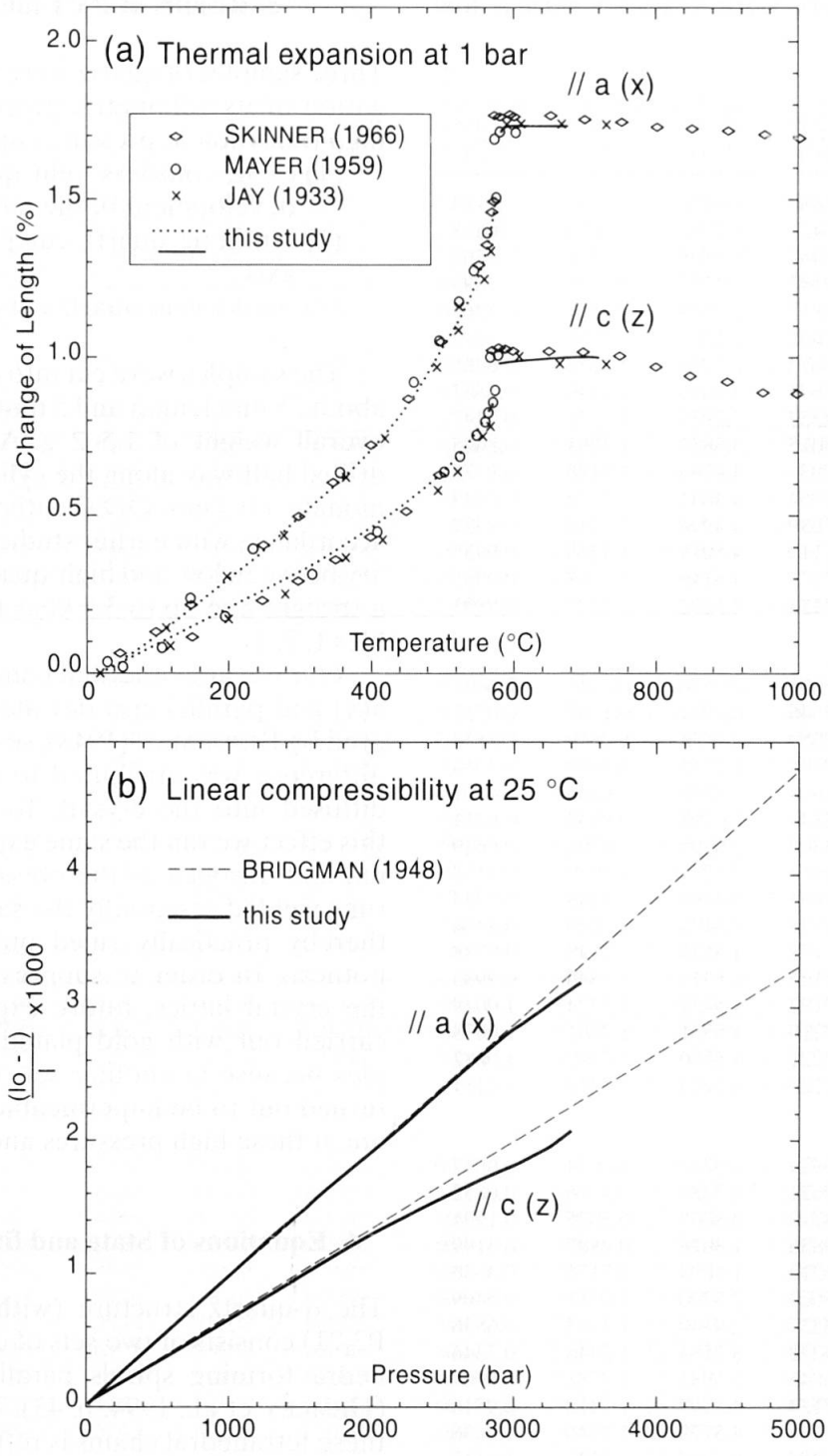

Fig. 3 A comparison of our measurements with other studies. For measurement errors see Tables 1 and 2 and text. (a) Isobaric thermal expansion of quartz at 1 bar (JAY, 1933; SKINNER, 1966; MAYER, 1959; see also ACKERMANN and SORRELL, 1974). (b) Isothermal linear compressibility of quartz at 25 °C (BRIDGMAN, 1948). For a discussion of the deviation to the data of BRIDGMAN (1948) see text chapter five.

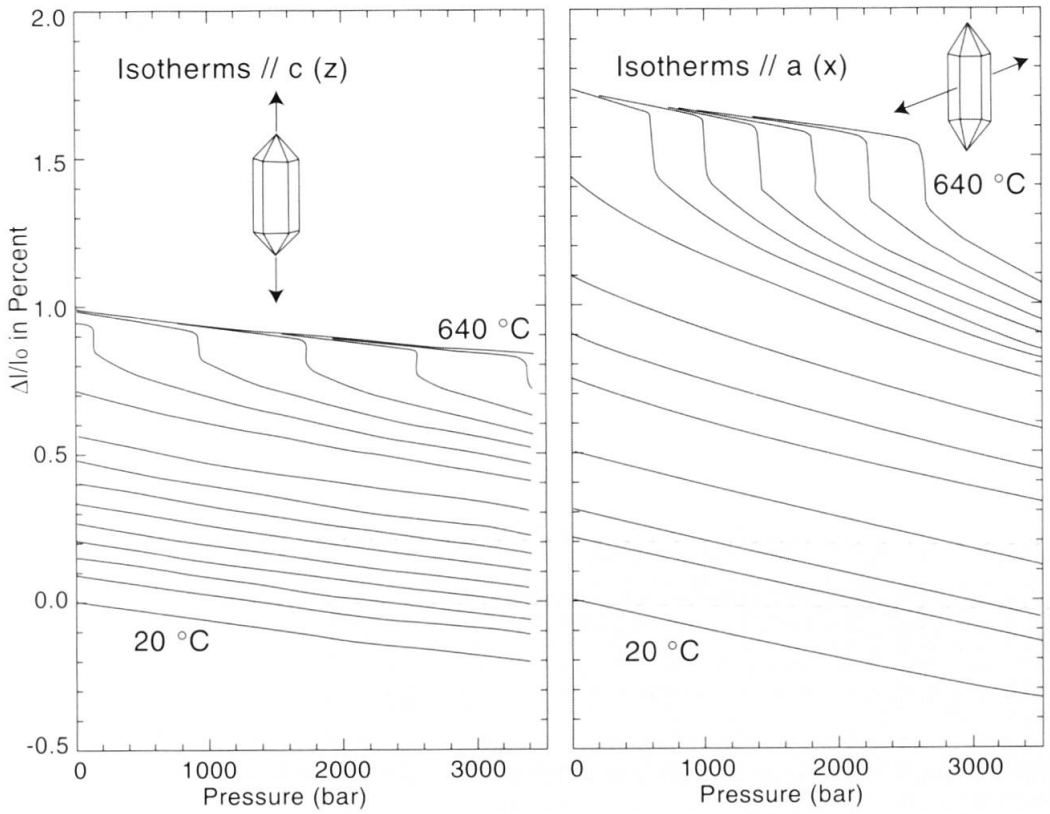

Fig. 4 Isothermal linear compressibility of quartz parallel to c(z) and a(x) axes at nominal temperatures between 20 °C and 640 °C. For precise temperatures and contour intervals see the corresponding Table 2 (//c(z) axis) and Table 3 (//a(x) axis).

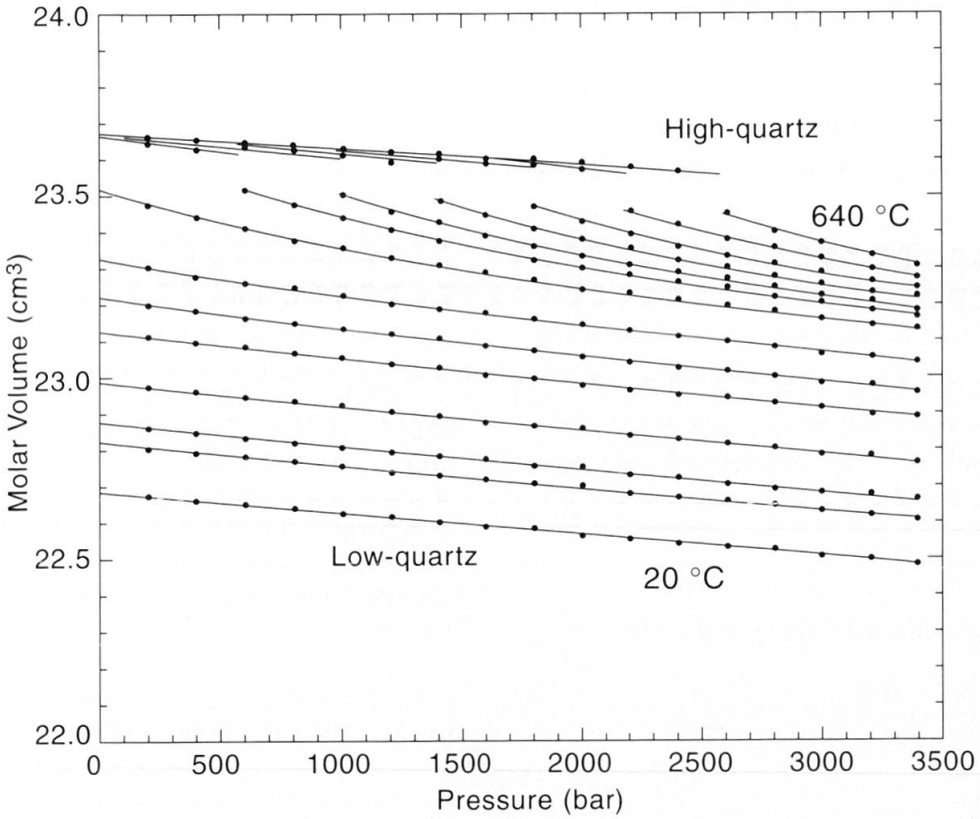

Fig. 5 Interpolated isothermal volume vs. pressure relationship of quartz at nominal temperatures from 20 °C to 640 °C and pressures up to 3500 bar as derived from Table 4. Data measured in isothermal decreasing pressure scans starting at 3500 bar and proceeding downwards to ambient pressure in approximately 5 bar steps. The low to high quartz transition is anticipated by gradually accelerated increase in molar volume.

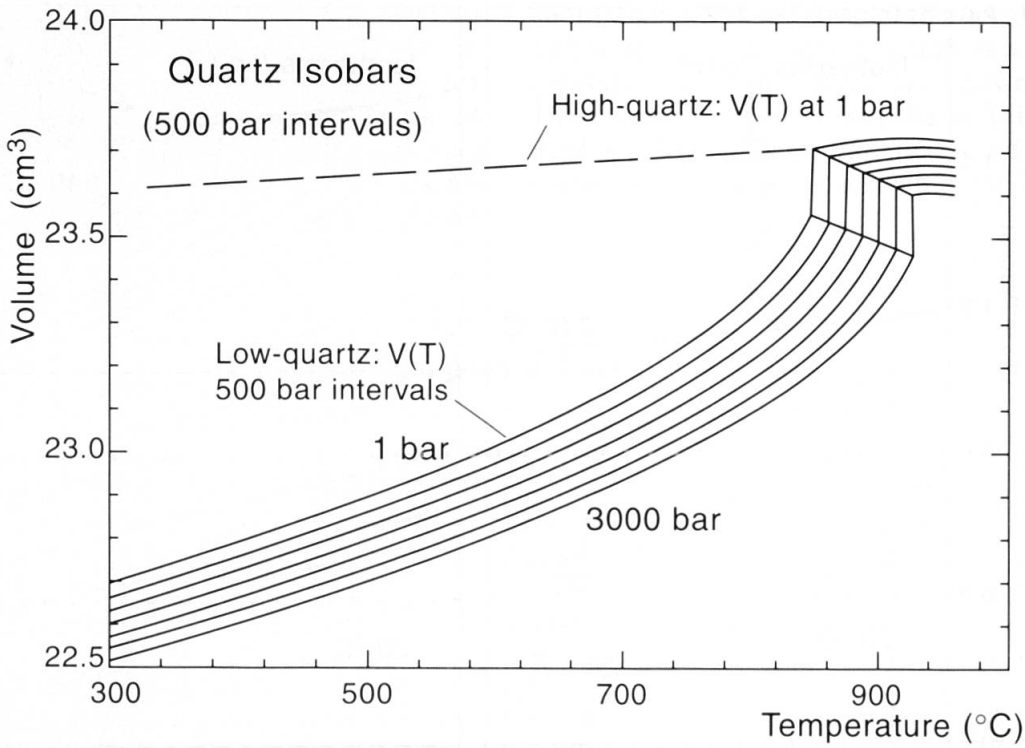

Fig. 6 Volumetric data for quartz as a function of temperature and pressure from 1 bar to 3 kbar (at 500 bar intervals). The volumetric data for high quartz has been extrapolated to lower temperatures, following the method of MAYER (1960), to determine ordering parameters.

6.1. EQUATIONS OF STATE FOR LOW (α-) QUARTZ

Most Equations of State (EOS) for volumetric changes as functions of P and T are modified from the van der Waals modification of the ideal gas law

$$(P + a/V^2)(V-b) = RT \quad (1),$$

for example to a virial equation of the form

$$V = Vo + a/P + b/P^2 + c/P^3 \quad (2).$$

In the present case, isothermal changes of pressure with volume were formulated as

$$V = Vo + AP + BP^2 \quad (3),$$

and isobaric changes with temperature as

$$V = Vo + AT + BT^2 \quad (4).$$

The best type of fitting for low-quartz data was obtained with

$$V(P,T) = A/(P + B) + CP^2 + DP + E \quad (5)$$

with

$$A = a_1T + a_2$$
$$B = a_3T^2 + a_4T + a_5$$
$$C = a_6$$
$$D = a_7T^2 + a_8T + a_9$$
$$E = a_{10}T^2 + a_{11}T + a_{12}.$$

The molar volume of 22.688 cm^3 at 1 bar and 298.15 K was taken from ROBIE et al. (1979). The molar volume data at T and P were fit to a function V = V(P,T) for low and high-quartz separately, the type and degree being the same for both (the number of adjustable parameters was minimized).

280 data points in the range from 1 to 3 kbar and 300 K up to T_c were taken as input for regression analysis. 3 additional points were calculated outside this limit by linear extrapolation to 200 K to improve the derivatives $(dV/dT)_P$ at the low temperature limit. The best fit constants (simplest equation with the lowest residuals) for low (α) quartz are:

a_1= 0.225007E+01	a_5= –0.208346E+04	a_9= –0.860444E–04
a_2= –0.997038E+03	a_6= 0.139958E–08	a_{10}= 0.631069E–06
a_3= –0.438645E–01	a_7= –0.792110E–10	a_{11}= 0.192899E–03
a_4= 0.430831E+02	a_8= 0.794849E–07	a_{12}= 0.226296E+02

with a sum of squares of 99.98107 and a standard deviation of 0.004 cm^3, where the maximum deviation is 0.015 cm^3.

6.2. CRYSTALLOGRAPHIC EOS FOR LOW (α) QUARTZ

The EOS presented here is purely empirical, based on isobaric and isothermal, as well as polythermobaric, analysis of the experimental data. The mathematical relations were chosen in a purely pragmatic manner. The aim was to keep the fit function as simple as possible and represent the measured data with acceptable precision. Data for low and high-quartz were fitted independently to the same equation. Consequently it is not recommended that our function be extrapolated to obtain PVT values far outside the P-T-area covered by our experiments.

Recent developments of Equations of State for volumetric changes as functions of P and T are to be found in the fitting of high-pressure lattice parameter data (e.g., ANGEL, 2000). These equations developed for solids have followed the Birch-Murgnaghan equations in terms of expressing volume changes as functions of pressure and bulk moduli (reciprocal compressibility). We have used the data fitting program of Angel on his website (http://www.geol.vt.edu/rja/soft/) to fit our data in Table 3 to obtain a series of isothermal Birch-Murgnaghan equations. The raw data may thus be used by any reader to obtain their own preferred fit equations. The Birch-Murnaghan equation

$$P = 3K_0 f_E(1 + 2f_E)^{5/2}\{1 + 3/2(K' - 4)f_E + 3/2 [K_0K'' + (K' - 4)(K' - 3) + 35/9]f_E^2\}$$

with $f_E = [(V_0/V)^{2/3} - 1)]/2$

was used to second order truncation (K'=4). Initial values of $V_0 = 22.6929 cm^3$ and $K_0 = 45 GPa$ were chosen. The resulting fitted values for V_0, K_0 and K'' are listed in Table 4 (note: K' is fixed to 4). The quality of the isothermal fit decreases rapidly with increasing temperature, reflecting the softening of low-quartz approaching the α-β phase transition.

Table 4 Fit parameters to a series of isothermal Birch-Murgnaghan equations obtained using the fitting routines of ANGEL (2000).

Temp [°C]	V_0 [cm³]	K_0 [GPa]	K' [ ]	K'' [GPa⁻¹]
25	22.69270	37.92129	4.0	–0.01026
100	22.76634	37.45919	4.0	–0.01038
200	22.87007	35.87710	4.0	–0.01084
300	22.98223	33.69838	4.0	–0.01154
400	23.11651	30.64829	4.0	–0.01269
500	23.29894	26.44702	4.0	–0.01470
520	23.34470	25.09329	4.0	–0.01550

6.3. EQUATIONS OF STATE FOR HIGH (β) QUARTZ

For high (β) quartz the same function (equation 5) was used for fitting and the following constants were obtained:

b_1= –0.440968E+00	b_5= –0.319299E+00	b_9= –0.247462E–02
b_2= 0.195727E+00	b_6= –0.383799E–09	b_{10}= –0.400260E–05
b_3= 0.678930E–01	b_7= –0.271121E–08	b_{11}= 0.742196E–02
b_4= 0.171344E+00	b_8= 0.513888E–05	b_{12}= 0.202996E+02

with a sum of squares of 97.38915 and a standard deviation of 0.005 cm^3, where the maximum deviation is 0.024 cm^3.

6.4. NEGATIVE THERMAL EXPANSION OF HIGH (β) QUARTZ

Our thermal expansion data show that high-quartz exhibits negative thermal expansion (i.e. high (β)-quartz shrinks when it is heated, see the recent discussion by WELCHE et al., 1998). Also our data show that the axial ratio c/a decreases from about 1.1001 at room temperature to a nearly constant value of about 1.092 above the transition temperature (RAZ, 1983, Fig. 46, p. 73). Similar observations were implied in earlier high temperature x-ray studies (ACKERMANN and SORRELL, 1974; JAY, 1933; BERGER et al., 1966) but are not visible in all fits of volumetric data (e.g., DOROGOKUPETS, 1995, Fig. 8, p. 8496). TUCKER et al., (2000a) have recently noted that the volume of high-quartz is lower than would be calculated from the actual Si–O bond lengths. This and other examples of lattice shrinking are interpreted by DOVE et al. (2000, p. 26) in terms of Rigid Unit Modes of linked polyhedra in framework structures.

More recent data, reviewed by CARPENTER (2000, p. 46, Fig. 8), indicate that it is the c(z)-direction which shows the principal negative thermal expansion, whereas the a(x)-direction shows little change or is slightly positive from their data. Our data show that the a(x)-direction shows weak negative thermal expansion.

6.5. RELATIVE MERITS OF THE DILATOMETER VS. DIAMOND ANVIL CELLS

In comparison to x-ray diamond anvil cell (DAC) studies, our dilatometric approach to PVT measurement suffers from a number of limitations but also offers features not known with DAC's. The major drawback certainly lies in the technical up-

per pressure limit of approx. 15 kbar to our technique. Proceeding beyond crustal conditions remains outside the realm of cold-seal bomb and internally heated pressure vessel dilatometry. On the other hand, resolution and accuracy of the dilatometry method are better. Thanks to the commercially available piezo-electric transducers and charge amplifiers, pressures in experimental apparatus may be resolved close to 1 ppm. The dilatometric technique fitted together with piezo-pressure sensors provides an extremely powerful method for the detailed study of phase transitions and their kinetics. A new future application, proposed here, will permit combination of our PVT data to DAC's driven by piezo-electric force actuators rather than by fine pitched mechanical screws.

7. Other physical properties reflecting these volumetric changes

MAYER (1960) measured the isobaric thermal expansion of quartz in both a(x) and c(z) directions at room pressure. He defined a parameter, like the ordering parameter in Landau theory, based upon the difference between the actual low-quartz volume at temperature and the down temperature extrapolated high-quartz volume, which has zero value above the transition temperature and tends towards infinity towards low temperature (RAZ, 1983, Fig. 45 p. 72). We have incorporated this method into the construction of Fig. 6. These data are consistent with results from Raman spectroscopic data of soft modes (HOECHLI and SCOTT, 1971; BACHHEIMER and DOLINO, 1977; BARRON et al., 1982), and from elastic constant measurements for compliance C_{14} (HOECHLI, 1970; AXE and SHIRANE, 1970, and the recent summaries in the volume edited by REDFERN and CARPENTER, 2000).

8. Open questions about Equations of State

The ease of fitting a mathematical function to a given data set depends upon the extent of its change. In our case this is reflected by the values of the partial first and higher derivatives (divergences in Fig. 3) of the volume function (compressibility $(\delta V/\delta P)_T$ and thermal expansion $(\delta V/\delta T)_P$). Various requirements may be of importance when choosing a mathematical relation to represent this function:

(a) best possible approximation to the measured data set,

(b) reflection of a known or assumed physical relation among the variables,

(c) and/or as a consequence of (b) the possibility of sound extrapolation beyond the measurement range of the data set.

Our polynomial functions were selected principally with requirement (a) in mind. We found that the fit parameters to a series of isothermal Birch-Murgnaghan equations (Table 4) were quite imprecise, even though they relate to requirements (b) and (c). Likewise, classical Equations of State are not adequate close to phase transitions (see DOROGOKUPETS, 1995). Within the P-T-range covered by our measurements, noticeable divergence from linearity occurs in the vicinity of the low to high-quartz phase transition. This feature anticipates the advent of the phase transition (Fig. 6). Unfortunately, a quantitative determination of onset points on the low side of the transition is not feasible with our technique.

While there is an attraction to the elegance of a known or assumed physical relation among the variables (requirement b above), we can rarely fulfill the expected simplicity. Today with the development of computer based mathematical tools we can present measured raw data in tables and interpolate them as needed. This can also be done for simple determination of derivatives and inversion of the function with respect to all variables, etc. Development of Equations of State (EOS) for extrapolation of data beyond the range of measurements will continue as remarked for requirement (c) above. Our PVT data may be used for testing EOS derived from ab initio calculations.

9. Applications and outlook

Our data have several applications involving the physical behaviour of quartz and other common minerals. Most studies of fluid inclusions in minerals assume rigid cavities which means that the volume and shape of the inclusions should not change during cooling and decompression. This simplification may now be corrected with our data for quartz.

A future application of our data concerns the method for calibrating and measurement in Diamond Anvil Cells. Our PVT data for quartz would permit piezo-electric force actuators to be used rather than the crude method of fine pitched mechanical screws as used at present.

Acknowledgements

The authors wish to thank Brigitte Bühlmann and Urs Graber for their engineering and technical support. We thank Ross Angel for supply his EOS program and for discussions about its application. We wish to thank

Michael Carpenter and A. Nonymous for reviewing the manuscript. This work was supported by ETH research credits.

References

ACKERMANN, R.J. and SORRELL, C.A. (1974): Thermal expansion and the high-low transformation in quartz. J. Appl. Cryst. C 7, 461–467.

ANGEL, R.J. (2000): Equations of state. In: HAZEN, R.M. and DOWNS, R.T. (eds): High-Temperature and High-Pressure Crystal Chemistry. Rev. Mineral. Geochem. 41, 35–59.

ANGEL, R.J., ALLAN, D.R., MILETICH, R. and FINGER, L.W. (1997): The Use of Quartz as an Internal Pressure Standard in High-Pressure Crystallography. J. Appl. Cryst. 30, 461–466.

ASLANIAN, T.A. and LEVANYUK, A.P. (1979): On the possibility of the incomensurate phase near α-β transition point in quartz. Solid State Communications 31, 547–550.

ASLANIAN, T.A. and LEVANYUK, A.P. (1984): Fluctuation effects as a cause for the incommensurate phase formation. Ferroelectrics 53, 231–234.

ASLANIAN, T.A., LEVANYUK, A.P., VALLADE, M. and LAJZEROWICZ, J. (1983): Various possibilities for formation of incommensurate superstructure near the α-β transition in quartz. J. Physics C 16, 6705–6712.

AXE, J.C. and SHIRANE, G. (1970): Study of the α-β quartz phase transformation by inelastic neutron scattering. Phys. Rev. B1, 342–348.

BACHHEIMER, J.P. (1980): An anomaly in the β phase near the α-β transition of quartz. J. Phys. Lett. 41, L559–L561.

BARRON, T.H.K., COLLINS, J.F., SMITH, T.W. and WHITE, G.K. (1982): Thermal expansion, Grueneisen functions and static lattice properties of quartz. J. Physics C 15, 4311–4326.

BASTIE, P., MOGEON, F. and ZEYEN, C.M.E. (1988): Direct neutron observation of a single-q incommensurate phase of quartz at zero stress. Physical Review B 38, 786–788.

BEALL, G.H. (1994): Industrial applications of silica. Rev. Mineral. 29, 468–505.

BERGER, C., EYRAUD, L., RICHARD, M. and RIVIERE, R. (1966): Etude radiocristallographique de variation de volume pour quelques matériaux subissant des transformations de phase solide–solide. Société Chimique de France Bulletin 1966, 628–633.

BRIDGMANN, P.W. (1948a): The compression of 39 substances to 100,000 kg/cm^2. Proc. Am. Acad. of Arts and Sciences 76, 55–70.

BRIDGMANN, P.W. (1948b): The compression of 39 substances to 40,000 kg/cm^2. Proc. Am. Acad. of Arts and Sciences 76, 71–87.

BYSTRICHOV, A.S. (1966): The nature of the low–high transformation in quartz. Geochem. International 1966, 223–229.

CARPENTER, M.A., SALJE, E.K.H., GRAEME-BARBER, A., WRUCK, B., DOVE, M.T. and KNIGHT, K.S. (1998): Calibration of excess thermodynamic properties and elastic constant variations due to the α–β phase transition in quartz. Am. Mineral. 83, 2–22.

COHEN, R.E. (1994): First-principles theory of crystalline SiO_2. In: HEANEY, P.J., PREWITT, C.T. and GIBBS, G.V. (eds): Silica – Physical Behavior, Geochemistry and Materials Applications. Rev. Mineral. 29,369–402.

D'AMOUR, H., DENNER, W. and SCHULZ, H. (1979): Structure determination of α-quartz up to 68 × 10^8 Pa. Acta Cryst. B35, 550–555.

DOLINO, G. (1990): The α-β transitions of quartz: A century of research on displacive phase transitions. Phase Transitions 21, 59–72.

DOLINO, G. and VALLADE, M. (1994): Lattice dynamical behavior of anhydrous silica. In: HEANEY, P.J., PREWITT, C.T. and GIBBS, G.V. (eds): Silica: Physical behavior, geochemistry and materials applications. Rev. Mineral. 29, 403–431.

DOROGOKUPETS, P.I. (1995): Equation of state for lambda transition in quartz. J. Geophys. Res. 100/B5, 8489–8499.

DREBUSHCHAK, V.A. and DEMENT'EV, S.H. (1993): Thermodynamic study of quartz in the vicinity of the α-β quartz transition. Geokhimia 9, 1341–1353.

GHIORSO, M.S., CARMICHAEL, I.S.E. and MORET, L.K. (1979): Inverted high temperature quartz. Contrib. Mineral. Petrol. 68, 307–323.

GLINNEMANN, J.J., SCHULZ, H.E.K., HAHN, T., PLACA, S.J.L. and DACOL, F. (1992): Crystal structures of the low-temperature quartz-type phases of SiO_2 and GeO_2 at elevated pressure. Z. Kristallogr. 198, 177–212.

HATTA, I., MATSUURA, M., YAO, H., GOUHARA, K. and KATO, N. (1985): True behaviour of heat capacity in α, incommensurate, and β phases of quartz. Thermochimica Acta 88, 143–148.

HAZEN, R.M., FINGER, L.W., HEMLEY, R.J. and MAO, H.K. (1989): High-pressure crystal chemistry and amorphization of α-quartz. Solid State Communications 72, 507–511.

HEANEY, P.J. (1994): Structure and chemistry of the low-pressure silica polymorphs. In: HEANEY, P.J., PREWITT, C.T. and GIBBS, G.V. (eds): Silica: Physical Behaviour, Geochemistry, and Materials Applications . Rev. Mineral. 29, 1–40.

HEANEY, P.J. (2000): Phase transformations induced by solid solution. In: REDFERN, S.A.T. and CARPENTER, M.A. (eds): Transformation processes in minerals. Rev. Mineral. Geochem. 39, 135–174.

HEANEY, P.J., PREWITT, C.T. and GIBBS, G.V. (1994): Silica: Physical behaviour, geochemistry and material applications Rev. Mineral. 29. Mineralocial Society of America, Washington, D.C., 606 pp.

HEANEY, P.J. and VEBLEN, D.R. (1991): Observations of the α-β transition in quartz: A review of imaging and diffraction studies and some new results. Am. Mineral. 76, 1018–1032.

HEMLEY, R.J., PREWITT, C.T. and KINGMA, K.J. (1994): High-pressure behavior of silica. In: HEANEY, P.J., PREWITT, C.T. and GIBBS, G.V. (eds): Silica: Physical Behaviour, Geochemistry, and Materials Applications. Rev. Mineral. 29, 41–81.

HOECHLI, U.T. (1970): Ultrasonic investigations of the first-order α-β phase transition of quartz. Solid State Communications 8, 1487–1490.

HOECHLI, U.T. and SCOTT, J.F. (1971): Displacement parameter, soft-mode frequency, and fluctuations in quartz below its α-β phase transistion. Phys. Rev. Lett. 26, 1627–1629.

JAY, A.H. (1933): The thermal expansion of quartz by x-ray measurements. Proc. Roy. Soc. A 142, 237–247.

KANEDA, R., YAMAMOTO, S. and NISHIBATA, K. (1971): Fixed Points on the High-Pressure Scale Identified by Phase Transitions in Ammonium Fluoride. In: Accurate Characterization of The High-Pressure Environment, Nat. Bur. Stand. (U.S.) Spec. Publ. 326, 257–262.

KEITH, M.L. and TUTTLE, O.F. (1952): Significance of variation in the high-low inversion of quartz. Am. J. Sci. Bowen Volume, 203–280.

KELLEY, K.K. (1960): Contributions to the data on theoretical metallurgy XIII. High temperature heat-con-

tent, heat-capacity, and entropy data for the elements and inorganic compounds. U.S. Bureau of Mines Bulletin 584, 232.

KINGMA, K.J., HEMLEY, R.J., MAO, H.K. and VEBLEN, D.R. (1993): New high-pressure transformation in α-quartz. Phys. Rev. Lett. 70, 3927–3930.

LEVIEN, L., PREWITT, C.T. and WEIDNER, D.J. (1980): Structure and elastic properties of quartz at pressure. Am. Mineral. 65, 920–930.

MAJUMDAR, A.J., MCKINSTRY, H.A. and ROY, R. (1964): Thermodynamic parameters for the alpha-beta quartz and alpha-beta cristobalite transitions. J. Phys. Chem. Solids 25, 1487–1489.

MALOV, Y.V. and SONYUSHKIN, V.E. (1976): Direct electron-microscopic investigation of the α-β transition process in quartz. Soviet Phys. Crystall., USSR 20-644-645

MAYER, G. (1960): Recherches expérimentales sur une transformation du quartz. Commissariat à l'Energie Atomique , C.E.A. 1330, 101.

MILETICH, R., ALLAN, D.R. and KUHS, W.F. (2000): High-pressure single-crystal techniques. Rev. Mineral. Geochem. 41, 445–519

OGATA, K., TAKÉUCHI, Y. and KUDOH, Y. (1987): Structure of α-quartz as a function of temperature and pressure. Z. Kristallogr. 179, 403–413.

PRYDE, A.K.A. and DOVE, M.T. (1998): On the sequence of phase transitions in tridymite. Phys. Chem. Minerals 26, 267–283.

RAMAN, C.V. and NEDUNGADI, T.M.R. (1940): The α-β transformation of quartz. Nature 145, 145–147.

RAZ, U. (1983): Thermal and volumetric measurements on quartz and other substances at pressures up to 6 kbars and temperatures up to 700 °C. Unpubl. PhD thesis ETH Zürich, nr. 7386, 91 pp.

REDFERN, S.A.T. and CARPENTER, M.A. (2000)(eds): Transformation Processes in Minerals. Rev. Mineral. Geochem. 39, 361 pp.

ROBIE, R.A., HEMINGWAY, B.S. and FISHER, J.R. (1979): Thermodynamic Properties of Minerals and Related Substances at 298.15 K and 1 Bar (10^5 Pascals) Pressure and at Higher Temperatures. Geol. Surv. Bull. 1452, 1–456.

SHAPIRO, S.M. and CUMMINS, H.Z. (1968): Critical opalescence in quartz. Phys. Rev. Lett. 21, 1578–1582.

SHEN, A.H., BASSETT, W.A. and CHOU, I.M. (1993): The α-β quartz transition at high temperatures and pressures in a diamond-anvil cell by laser interferometry. Am. Mineral. 78, 694–698.

SKINNER, B.J. (1966): Thermal expansions. In: CLARK, S.P. (ed.): Handbook of physical constants. Geol. Soc. Am. Mem. 97, 75–96.

SOSMAN, R.B. (1927): The properties of silica 37. The Chemical Catalog Company, New York, 856 pp.

STEINWEHR, H.E. (1932): Umwandlung α-β Quarz. Z. Kristallogr. 99, 292–313.

STULL, D.R. and PROPHET, H. (1971): JANAF thermochemical tables. 2nd ed. National Bureau of Standards NBS37. National Standards Ref. Data Series, 1141 pp.

TUCKER, M.G., DOVE, M.T. and KEEN, D.A. (2000b): Direct measurement of the thermal expansion of the Si–O bond by neutron total scattering. J. Physics Condensed Matter 12, L425–L430.

VALLADE, M., BERGE, B. and DOLINO, G. (1992): Origin of the incommensurate phase of quartz: II. Interpretation of inelastic neutron scattering data. J. Physics 2, 1481–1495.

VAN TENDELOO, G., VAN LANDUYT, J. and AMELINCKX, S. (1976): The α-β phase transition in quartz and $AlPO_4$ as studied by electron microscopy and diffraction. Phys. Status Solidi 33, 723–735.

WELCHE, P.R.L., HEINE, V. and DOVE, M.T. (1998): Negative thermal expansion in β-quartz. Phys. Chem. Minerals 26, 63–77.

YAKOVLEV, I.A., MIKHEEVA, L.F. and VELICHKINA, T.S. (1956): The molecular scattering of light and the α-β transformation in quartz. Soviet Phys. Crystall., USSR 1, 91–98.

YOUNG, R.A. (1962): Mechanism of the phase transition in quartz. US Air Force, Office of Scientific Research Contract No AF49(638)–624.

ZEYEN, C.M.E., DOLINO, G. and BACHHEIMER, J.P. (1983): Neutron and calorimetric observation of a modulated structure in quartz just above the α-β phase transition. Physica 120 B, 280–282.

Manuscript received April 26, 2002; revision accepted September 20, 2002.
Editorial handling: M. Engi